NASA TECHNICAL MEMORANDUM

NASA TM X-73425

NASA TM X-73425

OTW NOISE CORRELATION FOR VARIATIONS IN NOZZLE/WING GEOMETRY WITH 5:1 SLOT NOZZLES

by U. von Glahn and D. Groesbeck
Lewis Research Center
Cleveland, Ohio 44135

TECHNIC_ PAPER to be presented at
Third Aero-Acoustic Conference sponsored by the
American Institute of Aeronautics and Astronautics
Palo Alto, California, July 20-23, 1976

OTW NOISE CORRELATION FOR VARIATIONS IN NOZZLE/WING GEOMETRY WITH 5:1 SLOT NOZZLES

U. von Glahn* and D. Groesbeck**
National Aeronautics and Space Administration
Lewis Research Center
Cleveland, Ohio 44135

Abstract

Acoustic data obtained from a model-scale study with 5:1 slot nozzles are analyzed and correlated in terms of apparent noise sources. Variations in nozzle geometry include roof angle and sidewall cutback. In addition, geometry variations in wing size and flap deflection were included. Three dominant noise sources were evident in the data and correlated: fluctuating lift noise, trailing edge noise and a redirected jet mixing noise that included the effect of reflection of jet noise by the surface. Pertinent variables in the correlations included the shear layer thickness and peak jet flow velocity at the trailing edge.

Introduction

In order to help attenuate jet noise, designs for short takeoff and landing (STOL) aircraft with engines located over the wing (OTW) are being considered. Jet noise shielding by wings for STOL aircraft is reported in Refs. 1 to 8. These data generally were obtained with simple circular and slot nozzles. When the flaps were deflected to simulate landing or takeoff configurations, the nozzles tested, except for a 10:1 slot nozzle, had to be canted toward the wing surface or be equipped with an external flow deflector to promote flow attachment to the flap surfaces. Limited data on the importance of shielding surface length in the chordwise dimension has been reported in Ref. 3. These data showed that substantial increases in shielding benefits at high frequencies could be achieved with only modest increases in surface shielding length.

Another means of promoting flow attachment to a wing-flap system is by means of a nozzle having the upper portion of the nozzle or "roof" angled to cause the flow to impinge on the wing/flap surface, thereby promoting flow attachment to the surface.(9) Such nozzles can be considered to have an "internal deflector".

The present paper covers the correlation of acoustic results from a model-scale test program for nozzles with internal deflectors. Considered are the effect on the OTW acoustic characteristics of changes in nozzle roof (kickdown) and sidewall cutback angles, chord length, flap deflection, and location of the nozzle exhaust plane along the shielding surface (fig. 1). The test nozzles consisted of 5:1 slot nozzles with an equivalent diameter of 5.1 cm. Nozzle roof angles were varied from 10° to 40° relative to the wing chordline. The nozzle sidewalls in the exhaust plane were either normal to the shielding surface or cutback to be normal to the nozzle roof. Shielding surface lengths were varied nominally from 18 to 58 cm, and flap deflection angles of 20° to 60° were used. The nozzle exhaust plane was located at the nominal 21% chord station of the wing and at the beginning of the flap location (approximately 46% of the wing chord). The relative sizes of the nozzle to the various shielding surface lengths (fig. 2) simulate the effect of engine configurations on a twin engine aircraft, a siamese pod in which two engines exhaust from a single nozzle, and a single engine pod of a four-engine aircraft.

Acoustic data trends from this study are reported, in part, in Ref. 9 while the lift and thrust performance data are given in Ref. 10. The present paper is concerned with the correlation of the acoustic data of Ref. 9 in terms of the pertinent flow and geometry variables included in the test matrix. Acoustic data were taken only at 90° to the chordline of the airfoils. A nominal jet velocity of 266 m/sec was used to obtain aerodynamic and acoustic data for all test configurations. Acoustic data were also obtained at 200 m/sec.

Apparatus and Procedure

Facility

The aerodynamic and acoustic data used herein were obtained from noise tests conducted using an out-of-doors facility within the 7x15 m courtyard of a subsonic wind tunnel at the Lewis Research Center. This facility is described in Ref. 11. Open-cell foam pads were used to minimize reflections from the surrounding walls. In addition, foam pads were also placed on the ground to minimize ground reflection effects on the acoustic data.

Sound pressure level (SPL) spectra were obtained using a 1.27-cm diameter condenser microphone with wind screen. Data were recorded at 90° to the jet axis (90° to the airfoil chordline) at a microphone distance of 3.05 meters. The noise data were recorded on a FM tape recorder and digitized by a four second time averaged one-third octave band spectrum analyzer. The analyzer determined sound pressure level spectra in decibels referenced to 2×10^{-5} N/m^2.

Jet Mach number (velocity) profiles were obtained at the trailing edge of the shielding surfaces. Measurements were made with a traversing pitot tube with an entrance cone angle of 60° to help minimize flow angularity effects resulting from the jet flow over the curved surfaces. A vane on the traversing equipment was used to establish the jet flow angle for each traverse. When the flow angle, as determined by means of the vane, exceeded the angularity capability of the pitot tube, the tube angle to the local flow was adjusted to provide suitable data. The pressures measured were transmitted to an x-y-y' plotter which yielded direct traces on graph paper of the total pressure distribution across the jet.

Acoustic data were taken at nominal jet velocities of 200 and 266 m/sec while aerodynamic data were taken at a nominal jet velocity of 266 m/sec.

*Member AIAA; Chief, Jet Acoustics Branch
**Aerospace Research Engineer

Models

Nozzles. The test nozzles consisted of the 5:1 slot nozzles shown in figure 3 (see also ref. 9). The nozzles all had equivalent diameters of 5.1 cm. A single straight-sided nozzle was used for the tests without nozzle sidewall cutback (fig. 3(a)). The roof angle, β, for this nozzle was changed by providing inserts that altered the angle from 10° to 40° in 10° increments. Separate nozzles were provided for the cases with sidewall cutback (fig. 3(b) to 3(e)). The sidewall cutback angle, γ, was the same as the roof angle for each respective nozzle. The sidewalls of all these nozzles were parallel.

In addition to the nozzles just discussed a simple 5:1 slot nozzle (ref. 9) was used as the baseline nozzle (fig. 3(f)). Each of the sides of this nozzle converged at 5° and the nominal nozzle dimensions at the exhaust plane were 2.0 cm by 10.2 cm.

The nozzles are referred to by their roof and cutback angles; for example, the nozzle with a 20° roof angle and 20° sidewall cutback angle is designated by "20/20" while the nozzle with a roof angle of 20° and no sidewall cutback is designated by "20/0".

Wings. The wings (shielding surfaces) are shown schematically in figure 4 together with pertinent dimensions. The surfaces consisted of metal plates secured to wooden ribs (fig. 3). The surface approximated the upper surface contours of the airfoils with 20° and 60° deflected flaps used in Refs. 3 and 4.

All wings had a span of 61 cm. As indicated in figure 4, the nozzles were located at two axial locations on the surfaces corresponding to nominal airfoil chordwise stations of 21- and 46-percent with flaps retracted.

The wings will be referred to by the flap deflection angle, α, 20° or 60°, and their relative size given by 2/3-baseline, baseline and 3/2-baseline. The equivalent flaps-retracted chord sizes for these wings are 22, 33, and 49.5 cm respectively.

Noise Source Identification

In the present study, three primary noise sources are identified. These noise sources are shown schematically in figure 5 and consist of fluctuating lift noise (I), trailing edge noise (II) and a redirected jet-mixing noise source that includes the noise caused by reflections of acoustic waves from the wing/flap surface (III). Also shown in figure 5, for comparison, is a curve representing the nozzle-only noise. A brief discussion of the characteristics associated with these sources is given in the following sections.

Noise source I. The increase in noise level at low frequencies, compared with the nozzle only curve, is believed to be due to fluctuating lift. The large-scale turbulence structure of the jet flow field (ring vortices) is believed to be responsible for this fluctuating lift noise. McKinzie (ref. 12) postulates that this fluctuating lift noise can be represented by the peak jet velocity at the flap trailing edge and the shear layer thickness of the jet at this location; hence,

$$\text{Noise source I} \sim U_m^{\,6}\delta^4 \qquad (1)$$

Hayden (ref. 13) developed a similar relation, but varies the velocity exponent from 6 to 4 with increasing jet Mach number (subsonic flow). Because of its low frequency (particularly for full-scale), noise source I is normally not significantly shielded by practical wing/flap systems when considered in the light of barrier shielding experience (ref. 14).

Noise source II. In the mid-frequency range (fig. 5), noise source II is believed to be due to trailing-edge noise. A number of investigators concerned with OTW source noise modelling have developed analytical models to explain these data and provide means for source noise prediction. A brief summary of the pertinent analytical parameters believed to influence trailing-edge source noise given in the literature is summarized as follows. McKinzie (ref. 15) indicates that trailing edge source noise for engine under-the-wing configurations follows a $U_m^{\,5}\delta_{BL}$ relationship. Hayden (ref. 13) states that this source noise follows a $U_m^{\,6}\delta_{BL}$ relationship. Tam (ref. 16) indicates that the trailing-edge source noise originates in the wake downstream of the trailing edge and follows a $U_m^{\,6}\delta_{SL}$ relationship. Finally, Ffowcs Williams (ref. 17) believes that this source noise (II) follows a $U_m^{\,5}\delta_R$ relationship without specifically identifying the δ_R to be used as either the boundary layer or shear layer height, but considers it only as a characteristic height.

Unless flow separation occurs on the flap upstream of the trailing edge, it would appear that no shielding of trailing-edge noise by the flap should occur.

Noise source III. Noise source III (jet mixing noise) is postulated on the basis that the barrier shielding theory of Ref. 14 is adequate to predict the attenuation due to obstacles (wing) between the noise source and the observer. The emergence of this apparent high frequency mixing noise source became evident during the analysis of the present data. In a number of test configurations (as well as some reported in the literature (Refs. 3 and 17) the measured data were above the nozzle-only values although application of barrier shielding theory indicated that some acoustic shielding should have occurred. The fact that barrier shielding is based on a point source rather than a distributed source, as in the case of an exhaust jet, does not appear to account for this anomaly. Application of barrier theory to typical data from the present study indicates that at high frequencies, an effective mixing noise source exists at some level above that indicated by the nozzle-only data. Such a reconstitution of noise source III is shown schematically in figure 6. The spectral shape of this noise source is similar to that for a jet flowing parallel to the wing at the nozzle exhaust plane rather than the spectra associated with the test nozzle (nozzle with roof angle and with or without sidewall cutbacks). This implies that the wing/flap system redirects the flow, as would be expected, and that the jet mixing noise responds to this altered flow

path. Because of the flow path alteration, a change in turbulence level appears to occur that could account for the higher noise levels. Examination of earlier OTW data with a 10:1 slot nozzle for which acoustic measurements were made both above and below the wing (ref. 1) appear to substantiate these findings and indicate that a portion of the increased noise level for source III is due to acoustic reflections of the jet flow noise by the shielding surface. From practical considerations, mixing noise source III may be the only noise source that is attenuated by the shielding benefits derived from the presence of the wing/flap system when the flow is firmly attached to the wing/flap system.

Data Analysis

In the present paper, the noise sources are analyzed in terms of the prime variables that determine the peak SPL values for noise sources I and II and the associated changes in the respective frequencies for the peak SPL values. These prime variables include consideration of: characteristic shear layer height, jet velocity, peak velocity at the trailing edge, effective nozzle height and area, wing/flap surface length, etc.

Data Trends

Typical variations of peak SPL for both noise sources I and II as a function of a characteristic shear layer height are shown in figure 7. The characteristic shear layer height used herein is that for 0.5 U_m. With increasing surface length, the characteristic shear layer height increases (essentially directly with surface length for the wing/flap sizes used). Furthermore, with decreasing jet Mach number, the peak SPL values decrease; at the same time the characteristic shear layer height appeared to increase approximately with $1/\sqrt{1 + M_j}$ for the range of M_j values used. The peak SPL also decreased with increasing nozzle roof angle. These trends were similar for nozzles both with and without sidewall cutback. The absolute values of the changes, however, were greater for those nozzles with sidewall cutback than those without.

In the determination of the effective jet mixing noise source III, prime variables similar to those used in the analysis of noise sources I and II were considered. The effective mixing noise source III spectra were determined by adding the attenuated noise (ΔdB) from barrier shielding to the measured SPL values at all frequencies greater than those associated with noise source II. In general, and as discussed earlier, the resultant spectra were curves parallel to the baseline 5:1 slot nozzle spectrum rather than that for the test nozzle being analyzed. The nozzle-only spectra are shown in figure 8 for the baseline 5:1 slot nozzle and several representative nozzles with various roof angles and with and without sidewall cutback. The spectral shapes are somewhat similar; however, the nozzles with sidewall cutback were noisier than those without sidewall cutback. This was due to the greater turning angle for these nozzles with sidewall cutback which in turn produced a greater directivity angle relative to the fixed 90° microphone with which the noise data were taken. In all cases the baseline 5:1 slot nozzle yielded the lowest nozzle-only noise.

Data Normalization

Characteristic dimension, δ^*. The present analysis indicated that noise sources I and II were a function of the shear layer height, δ_e. The term δ_e is defined as the shear layer height of the free jet boundary measured at the trailing edge where the local velocity is 0.5 that of the peak velocity, U_m. This height is then normalized for the increase necessitated for equal weight flow by adjusting the nozzle size to the ratio of W_i/W. Thus, the characteristic height, δ^* is given by:

$$\delta^* = \delta_e + h \cos\gamma\sqrt{\frac{W_i}{W} - 1} \qquad (2)$$

The δ_e-term was obtained from trailing-edge velocity contours (ref. 9) for a nominal jet Mach number of 0.8. The δ_e-term for a nominal jet Mach number of 0.6 was obtained from the $M_j = 0.8$ data by:

$$\delta_e(1 + M_j)^{0.5} \quad @\ M_j = 0.6 \qquad = \delta_e(1 + M_j)^{0.5} \quad @\ M_j = 0.8 \qquad (3)$$

This relationship was verified by spot checks of the effect of jet Mach number on δ_e for several configurations.

Effective nozzle height, h^*. The effective nozzle height, h^* is defined as the actual nozzle height, h, normalized to yield ideal flow by increasing the nozzle height. For the present configurations, the h^*-term is given by:

$$h^* = h \cos\gamma\left(\frac{W_i}{W}\right)^{0.5} \qquad (4)$$

The increased nozzle height, of course, increases the nacelle drag in flight.

Correlation of Source Noise

In the present paper, the noise sources are assumed uncorrelated and thus their combined sound field can be approximated by superposition. Independent correlations were developed for the peak SPL values of each of the noise sources in terms of the prime variables. The latter include the peak jet flow velocity at the flap trailing edge, a characteristic dimension, jet exhaust velocity, and nozzle geometric variables such as roof angle, sidewall cutback angle, and nozzle height. Spectral shapes for the various noise sources were obtained from the data and finally the frequencies associated with the peak SPL values were correlated.

Noise Source I - Fluctuating Lift Noise

The correlated source noise for the fluctuating lift noise is shown in figure 9. The ordinate consists of: (1) the peak SPL value for noise source I; (2) the ratio of the jet exhaust velocity, U_j, to the peak flow velocity measured at the trailing edge, U_m, (ref. 10) raised to an exponent, m; (3) a corrected nozzle exhaust flow area, A_c; and (4) the jet exhaust velocity raised to an exponent, n. The abscissa consists of (1) the effective layer height, δ^*; (2) the effective nozzle

height, h^*; and (3) terms accounting for the nozzle roof angle, β, and nozzle sidewall cutback angle, γ.

Examination of the data showed that the m-exponent, for the velocity ratio U_j/U_m varied with the jet exhaust Mach number as suggested by Hayden (ref. 13). A variation of m with M_j was empirically obtained, within the limits given in Ref. 13 (6.0 for M_j values less than about 0.5 and 4.0 for M_j values near 1.0), and is expressed as follows:

$$m = 10 - 4\left[1 + 0.5\left(\frac{1}{1 + 0.1/M_j^8}\right)\right] \qquad (5)$$

For the data herein, values of m are 5.70 and 4.72 for M_j values of 0.602 and 0.803, respectively.

The noise level also varied with the fourth power of the jet exhaust velocity (U_j^4).

As discussed in Ref. 10, because of back pressure on the flow system caused by the nozzle roof angle and the presence of the wing/flap system, the data are normalized on the basis of equal flows. Thus, all the nozzle exhaust areas are increased by the ratio of the calculated ideal flow to the measured flow; W_i/W.

The ordinate in figure 9 for the present configurations is given by the following equation:

$$SPL^*_{I,p} = SPL_{I,p} + 10\,m \log \frac{U_j}{U_m} + 10 \log \frac{W_i}{W} - 40 \log - 40 \log U_j - 10 \log A \qquad (6)$$

After consideration of the various characteristic dimensions for use in correlating the data, it was determined that δ^*, a characteristic shear layer height, shown in the abscissa of figure 10 yielded the best correlation of the data. The characteristic dimension δ^* was nondimensionalized by dividing it by the effective nozzle height h^*.

The final terms in the abscissa consist of the effects of nozzle roof and sidewall angles on the peak SPL values. These terms are given by $(2 - \cos\beta)(1 + \sin^3\gamma)$. The slope of the curve shown faired through the data in figure 9 has an exponent of 4. It should be noted that the correlation is independent of the flap angle, α. Good correlation of the data are evident for the 20° flap angle (figs. 9(a) and 9(b)). With a 60° flap angle (fig. 9(c)) a large deviation in the data is apparent. Only the data for the 2/3-baseline wing correlate on the same curve (solid line) as that for the 20° flap angle. With increasing wing size, the more the data moved to the right of the correlation curve (solid line). The lack of correlation is believed due to the partial separation of the flow from the surface at the 60° flap angle. (A brief discussion of the effect of flap angle on flow patterns is given in Appendix A.) Thus, it is believed that aerodynamic measurements at the trailing edge are inappropriate to characterize fluctuating lift noise when the flow is partially separated as is the case for the 60° flap angle. In order to provide meaningful data the aerodynamic measurements should be made on the wing/flap surface near the flow separation region discussed in Appendix A. This would lead to lower δ^* and U_j/U_m values than those measured at the trailing edge and shift the data to the left toward the correlation curve (solid line) in figure 9(c).

Noise Source II - Trailing Edge Noise

The results of correlating the peak SPL values for source II, trailing-edge noise, are shown in figure 10. The ordinate consists of the measured peak SPL for each test condition and several flow and geometry parameters that influence that noise level. A nozzle flow area correction term was again employed in order to compare the data on the basis of equal flow rates. This term, as in the case of noise source I, is given by 10 log W_i/W. The correlation of the peak SPL was also a function of the peak local velocity at the trailing edge, U_m. This term is expressed in the ordinate by 50 log U_j/U_m. Thus, the velocity exponent relationship suggested by Ffowcs Williams in Ref. 17 yielded the best correlation with the peak trailing-edge velocity. The level of the peak SPL also varied with about the 8th-power of the jet velocity, U_j. Finally, in order to scale the data to larger nozzles (of the same shape) a nozzle area term is included. The ordinate in figure 10 is summarized by the following equation:

$$SPL^*_{II,p} = SPL_{II,p} + 10 \log W_i/W + 50 \log U_j/U_m - 80 \log U_j - 10 \log A \qquad (7)$$

The abscissa in figure 10 is simply the ratio of δ^*/h^* with no additional terms needed to account for changes in the nozzle roof and sidewall cutback angles (β and γ, respectively) and the flap deflection angle, α. The characteristic dimension δ^* is analogous to the undefined eddy height or size suggested in Ref. 17.

As part of the analysis, the shielding surface length and the boundary layer height at the trailing edge were also considered as candidates for the characteristic dimension. Both of these candidates are grossly related to δ^*; however, the best overall data fit was provided by the use of δ^*.

It should be noted that the data correlation for noise source II with a 60° flap angle (fig. 10 (c)) contains more data scatter than that with a 20° flap angle. This scatter is believed due to the partial flow separation encountered with the 60° flap angle.

Noise Source III - Redirected Jet Mixing Noise

The correlation of the redirected jet mixing noise, including reflections from the shielding surface, is shown in figure 11. The ordinate of figure 11 consists of the reconstatuted SPL discussed previously and the same general parameters included in the ordinates for noise sources I and II (figs. 9 and 10). The exponent for the ratio of U_j/U_m was determined to be 4.0 while the n-exponent for the jet velocity, U_j, was determined to be 8.0. The $SPL^*_{III,p}$ is given by the following equation:

$$SPL^{*}_{III,p} = SPL_{III,p} + 40 \log \frac{U_j}{U_m} + 10 \log \frac{W_j}{W}$$

$$- 80 \log U_j - 10 \log A + 20 \log (1 + \sin^2 \alpha) \quad (8)$$

The best form of the abscissa terms for correlation was determined to be δ^*/h^* multiplied by geometry functions expressed as $(2 - \cos \beta)(1 + \sin^{3/2} \gamma)/(1 + \sin^2 \alpha)$. The correlation for the 20° flap angle shows somewhat more data scatter for the nozzles with sidewall cutback (fig. 11(b)) than for those without sidewall cutback.

With a 20° flap angle, the reconstituted jet mixing noise spectral curves were up to 10 dB higher for the 2/3-baseline wing than those measured for the baseline 5:1 slot nozzle only; the difference decreased with increasing wing size, depending also on the nozzle used. The reconstituted jet mixing noise spectral curves for a 60° flap angle generally were only about 2-3 dB greater overall than those measured for the baseline 5:1 slot nozzle only. An anomaly to these general data trends occurred with the 60° flap angle and the 2/3-baseline wing. For this combination, the reconstituted spectra was not parallel to either the baseline 5:1 slot nozzle or the test nozzle but rather crossed the two spectral shapes. It is believed that this result was due to the particular flow situation existing over the wing/flap system with the nozzles used.

Frequency at Peak SPL

The frequencies associated with the peak SPL values for the various nozzle-wing configurations were correlated in terms of modified Strouhal numbers for each noise source. The parameters used for the correlations are the measured values of δ_e and h; however, in order to obtain the frequencies for the configurations adjusted to equal weight flows merely requires the substitution of δ^* and h^* for δ_e and h, respectively.

Noise source I. The modified Strouhal number for noise source I was found to be dependent on the shielding surface length, ratio of the peak velocity at the trailing edge to the jet exhaust velocity, ratio of δ_e/h, flap angle, and nozzle geometry variables. The following equation resulted in an approximation of the measured data:

$$ST_{I,p} = 0.09 = \frac{f_{I,p} L}{C_a} \left(\frac{U_j}{U_m}\right)^{2.5} \left(\frac{h}{\delta_e (2 - \cos \beta)(1 + \sin^{3/2} \gamma)}\right)^2 (1 + \sin^2 \alpha) \quad (9)$$

An exponent of 2.0 for the (U_j/U_m)-term was also satisfactory (with an appropriate adjustment to the Strouhal constant) for the 2/3-baseline and baseline wings data; however, the 3/2-baseline wing data were significantly lower than the resultant correlation curve. As in the case for the correlation of the peak SPL values for noise source I, Eq. (9) fails to correlate the 60° flap angle frequency data for the baseline and 3/2-baseline wings. The failure is again attributed to flow separation off the wing/flap surface and the consequent excessive δ_e-values.

Noise source II. The modified Strouhal number for noise source II was found to be dependent on nearly the same variables as those for noise source I. The main differences being that noise source II was independent of the velocity ratio U_j/U_m, whereas noise source I showed such a dependency. The best overall correlation of the frequencies associated with the peak SPL values were obtained with the following Strouhal relationship:

$$ST_{II,p} = 1.36 = \frac{f_{II,p} L}{C_a} \sqrt{\left(\frac{h}{\delta_e}\right) \frac{(1 + \sin \alpha)^2}{(2 - \cos \beta)(1 + \sin^3 \gamma)}} \quad (10)$$

It should be noted that much of the frequency data for the 2/3-baseline and baseline wings showed a weak dependency on U_j whereas the 3/2-baseline wing data did not show such a dependency. Assuming that the 3/2-baseline wing data is affected by flow separation, and that the weak U_j dependency is real, Eq. (10) should be rewritten as:

$$ST_{II,p} = 1.54 = \frac{f_{II,p} L}{U_j} \sqrt{\left(\frac{U_j}{C_a}\right) \frac{h(1 + \sin \alpha)^2}{\delta_e (2 - \cos \beta)(1 + \sin^3 \gamma)}}$$

The effect of U_j on the frequency amounts to only about 1/2 of a one-third octave band (about 15%) for a change in M_j from 0.6 to 0.8. As in the case of noise source I, the use of δ^* and h^* in place of δ_e and h, respectively is valid.

Spectral Shape

On the basis of the data accumulated in this study spectral shapes were determined to fit the spectra associated with both noise sources I and II. These spectral shapes are shown in figure 12. The spectral shapes are referenced to the peak frequency associated with the peak SPL values for noise sources I and II.

The shape of the baseline 5:1 slot nozzle spectrum, shown previously in figure 8, is used for the reconstituted jet mixing spectra for noise source III. The peak noise level for noise source III occurs at the same frequency as that for the nozzle-only spectrum (approximately 4000 Hz).

Prediction of Acoustic Spectra

The prediction of acoustic spectra for OTW configurations using the nozzles described herein is procedurally similar to that given in Ref. 18. The noise sources are assumed uncorrelated and thus their combined sound field can be approximated by superposition. A brief outline of this method follows together with schematic sketches illustrating the procedures.

Step 1. Plot the nozzle-only spectrum for the baseline 5:1 slot nozzle, determined by test or analysis, in terms of SPL as function of frequency (fig. 13(a)).

Step 2. The peak SPL value is then obtained for noise sources I and II (figs. 9 and 10, respec-

tively) and plotted at the appropriate frequency for each source as in figure 13(b). The appropriate spectral shape from figure 12 is then added.

Step 3. The baseline 5:1 slot nozzle spectrum level is increased according to the noise source III correlation given in figure 11, with the new spectrum shape for this noise source (reconstituted jet mixing noise) being parallel to that for the original baseline 5:1 slot nozzle spectrum (fig. 13(c)). The acoustic attenuation from the barrier shielding theory is then applied to the reconstituted jet mixing noise spectra as shown in figure 13(c).

Step 4. The final combined nozzle/wing, together with the baseline and test nozzle spectra are shown in figure 13(d). It is apparent, of course that if the measured data used to obtain the correlation curves fall on the curves good agreement must result. However, even in the cases shown where poor agreement exists between the measured data and the correlation curves, the predicted spectra are not significant in error since much of the measured SPL data fall within a ± 1.5 dB scatterband and the measured frequencies associated with the peak SPL values are within, at least, 1/2 of one-third octave band of the correlation values.

Concluding Remarks

The results presented herein appear to indicate that with an OTW configuration, only the redirected jet mixing noise, including acoustic reflection of this mixing noise from the wing/flap surface, is shielded by the wing/flap system. With attached flow, the noise associated with jet flow over the trailing edge is not shielded by the wing/flap system nor is the noise associated with fluctuating lift. In order to achieve significant improved jet/flap interaction noise reductions, trailing edge noise must be substantially attenuated, if not eliminated. One means to accomplish this is to use a longer shielding surface, a solution that in many cases does not appear practical. Use of porous trailing edge techniques, properly applied could yield some noise attenuation at model scale. However, at full scale the trailing-edge noise source frequencies would be relatively low and may be difficult to attenuate with practical techniques while still preserving good aerodynamic characteristics for the wing/flap system. A more promising attenuation method for reducing trailing edge noise would be to reduce the flow velocities just upstream of the trailing edge. This would significantly reduce the U_j/U_m terms in noise sources I and II and thereby reduce both the fluctuating lift and trailing edge noise. Means for obtaining such a reduction in trailing edge velocities could consider the use of vortex-generator-type devices upstream of the trailing edge. Such devices could be set to diverge the flow prior to the trailing edge thereby reducing the flow velocity and also reducing trailing edge noise. The expected high frequency noise generated by the vortex-generator-type devices would not appear to be of a magnitude to cause acoustic problems. In addition, that portion of the wing/flap surface downstream of the devices would help to shield this high frequency noise. For cruise operation, the devices could be retracted into the wing/flap surface.

Appendix A - Flow Visualization

Limited flow visualization studies were made in order to evaluate in a qualitative manner the degree of flow attachment for some of the nozzle/wing configurations. The method used was to inject a small stream of water (0.16 cm diameter tube) into the jet flow at the nozzle exhaust plane. The point of injection was made at various locations around the perimeter of the nozzle. In figure 14 representative overall flow patterns, obtained by visually observing the water streamers on the wing/flap surface with an M_j of 0.8, are sketched to indicate the primary patterns observed. With a 20° flap deflection, most nozzle configurations provided a widespread, well-attached flow pattern as indicated by the dash lines in the figure. With a 60° flap deflection, the surface flow pattern just downstream of the nozzle exhaust plane tended to spread out more than with the 20° flap deflection, as shown by the dashed curves in figure 14. With nozzle configurations for which the jet flow appeared to be partially detached from the surface (Region A) the flow pattern curved inward toward the centerline very rapidly, as shown by the dash-dot lines in figure 14, and left the flap trailing edge concentrated in a narrow region.

Nomenclature

(All data are in SI Units)

A	nozzle exhaust area
A_c	corrected nozzle exhaust area
C_a	ambient speed of sound
f	frequency
h	measured nozzle sidewall height
h*	normalized nozzle height
ℓ	wing chord length upstream of nozzle exhaust plane
L	shielding surface length
L_s	projected shielding length parallel to wing chordline
M_j	jet exhaust Mach number
m	exponent defined in text (Eq. (15))
n	jet exhaust velocity exponent
R	distance from noise source to microphone
SPL*	normalized SPL, defined in text
SPL	sound pressure level, dB re 2×10^{-5} N/m^2
ΔSPL	SPL - SPL_N, dB
ST	Strouhal number
u	local jet velocity at flap trailing edge
U_j	jet exhaust velocity
U_m	maximum velocity at trailing edge of flap
W	weight flow
Y,x,y	wing surface contour dimensions (see fig. 4)
α	flap deflection angle
β	nozzle roof angle
γ	nozzle sidewall cutback angle

δ	shear layer thickness of flap trailing edge
δ_e	shear layer thickness where $U = 0.5\ U_m$
δ^*	characteristic shear layer thickness dimension
I,II,III	noise source identifications

Subscripts

BL	boundary layer
i	ideal
m	maximum
N	nozzle
p	peak
R	arbitrary flow layer characteristics
SL	shear layer
I,II,III	noise sources

REFERENCES

1. Reshotko, M., Olsen, W. A., and Dorsch, R. G., "Preliminary Noise Tests of the Engine-Over-the-Wing Concept. I. 30°-60° Flap Position," NASA TM X-68032, Mar. 1972.

2. Reshotko, M., Olsen, W. A., and Dorsch, R. G., "Preliminary Noise Tests of the Engine-Over-the-Wing Concept. II. 10°-20° Flap Position," NASA TM X-68104, June 1972.

3. von Glahn, U., Reshotko, M., and Dorsch, R., "Acoustic Results Obtained with Upper-Surface-Blowing Lift-Augmentation Systems," NASA TM X-68159, 1972.

4. Dorsch, Robert G., Reshotko, Meyer, and Olsen, William A., "Flap Noise Measurements for STOL Configurations Using External Upper Surface Blowing," AIAA Paper 72-1203, NASA, New Orleans, La., 1972.

5. Reshotko, M., Goodykoontz, J. H., and Dorsch, R. G., "Engine-Over-the-Wing Noise Research," AIAA Paper 73-631, Palm Springs, Calif., 1973.

6. Dorsch, R. G., "Externally Blown Flap Noise Research," SAW Paper 740468, Dallas, Tex., 1974.

7. Olsen, W. and Friedman, R., "Noise Tests of a Model Engine-Over-the-Wing STOL Configuration Using a Multijet Nozzle with Deflector," NASA TM X-2871, Aug. 1973.

8. Reshotko, M. and Friedman, R., "Acoustic Investigation of the Engine-Over-the-Wing Concept Using a D-Shaped Nozzle," AIAA Paper 73-1030, Seattle, Wash., 1973.

9. von Glahn, U. and Groesbeck, D., "Geometry Effects on STOL Engine-Over-the-Wing Acoustics with 5:1 Slot Nozzles," NASA TM X-71820, 1975.

10. von Glahn, U., and Groesbeck, D., "Nozzle and Wing Geometry Effects on OTW Aerodynamic Characteristics," AIAA Paper 76-622, Palo Alto, Calif., 1976.

11. von Glahn, U. and Groesbeck, D., "Acoustics of Attached and Partially Attached Flow for Simplified OTW Configurations With 5:1 Slot Nozzle," NASA TM X-71807, 1975.

12. McKinzine, D., Burns, R., and Wagner, J., "Noise Reduction Tests of Large-Scale-Model Externally Blown Flap Using Trailing Edge Blowing and Partial Flap Slot Covering," NASA TM X-3379, 1976.

13. Hayden, R. E., "Noise from Interaction of Flow with Rigid Surfaces: A Review of Current Status of Prediction Techniques," NASA CR-2126, Oct. 1972.

14. Beranek, L. L., Noise Reduction, McGraw-Hill Book Co., New York, 1960, pp. 193-194.

15. McKinzie, D. and Burns, R., "Analysis of Noise Produced by Jet Impingement Near the Trailing Edge of a Flat and a Curved Plate," NASA TM X-3171, Jan. 1975.

16. Tam, C., "Trailing-Edge Noise," AIAA Paper 75-489, Hampton, Va., 1975.

17. Ffowcs Williams, J. E. and Hall, L. H., "Aerodynamic Sound Generation by Turbulent Flow in the Vicinity of a Scattering Half Plane," Journal of Fluid Mechanics, Vol. 40, Mar. 1970, pp. 657-70.

18. von Glahn, U., Groesbeck, D., and Reshotko, M., "Geometry Considerations for Jet Noise Shielding with CTOL Engine Over-the-Wing Concept," AIAA Paper 74-568, Palo Alto, Calif., 1974.

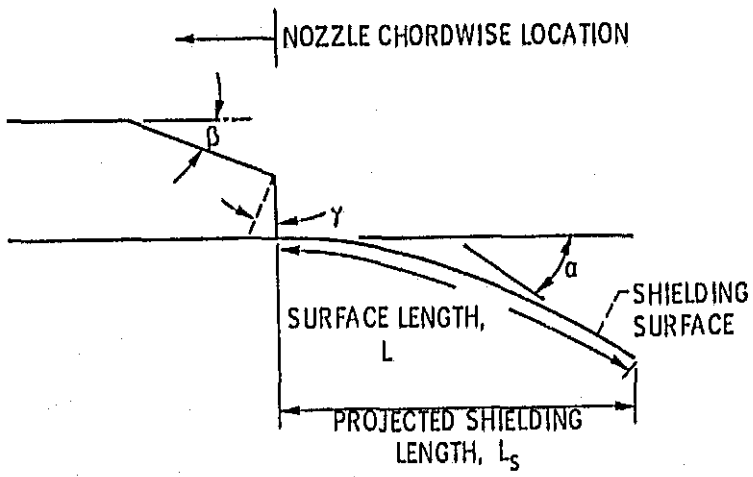

Figure 1. - Schematic sketch showing nozzle-wing/flap geometry elements varied in study.

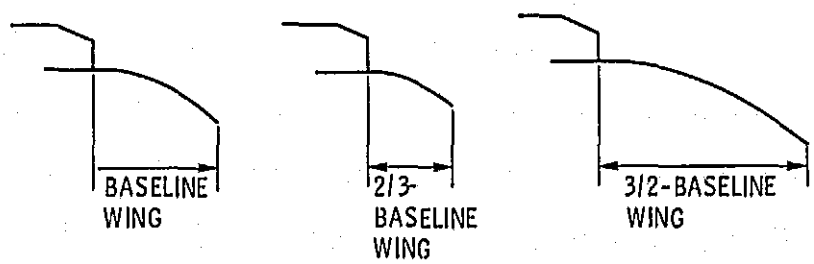

(a) BASELINE MODEL (TWIN-ENGINE AIRCRAFT).

(b) SIAMESE POD (COMMON EXHAUST).

(c) MULTIPLE POD (4-ENGINES).

Figure 2. - Aircraft configurations simulated by nozzle/wing test models.

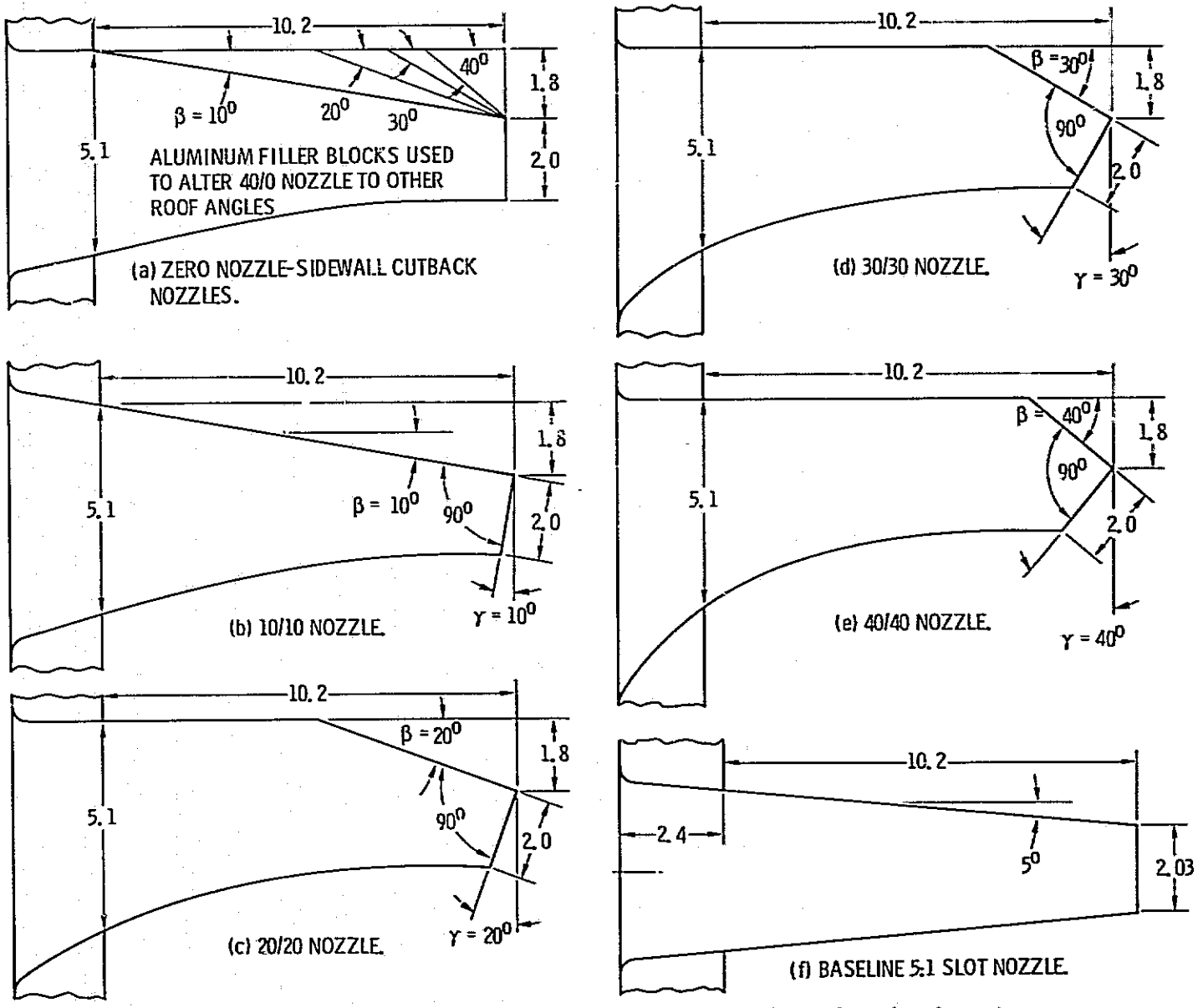

Figure 3. – Sketches of test nozzles; all nozzles were 10.2 cm wide. (Dimensions in cm.)

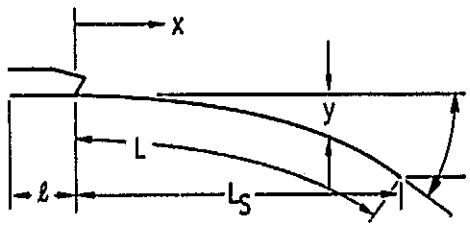

WING COORDINATES

FLAP ANGLE, α, DEG	WING CONFIGURATION	x/L_S / y/Y	0-0.4	0.5	0.6	0.7	0.8	0.9	0.95	0.975	1.0
20 60	2/3-BASELINE, BASELINE		0	0.04	0.13	0.26	0.44	0.70	0.85	-----	1.0
	3/2-BASELINE		0	0.025	0.10	0.225	0.42	0.7	0.85	-----	1.0
60	ALL		0	0.02	0.055	0.125	0.24	0.44	0.61	0.76	1.0

WING DIMENSIONS

FLAP ANGLE, α, DEG	CONFIGURATION	Y, CM	ℓ, CM	L_S, CM	L, CM
20	2/3-BASELINE	4.4 4.4	4.6 10.2	22.5 16.9	23.3 17.8
	BASELINE	6.6 6.6	6.9 15.2	33.8 25.4	35.4 27.0
	3/2-BASELINE	10.2 10.2	10.2 22.9	50.8 38.1	53.2 40.6
60	2/3-BASELINE	9.6 9.6	4.6 10.2	20.3 14.7	25.7 20.3
	BASELINE	14.3 14.3	6.9 15.2	30.5 22.1	38.7 30.2
	3/2-BASELINE	21.5 21.5	10.2 22.9	45.7 33.1	57.6 45.1

Figure 4. - Wing dimensions and coordinates. Dimensions in centimeters.

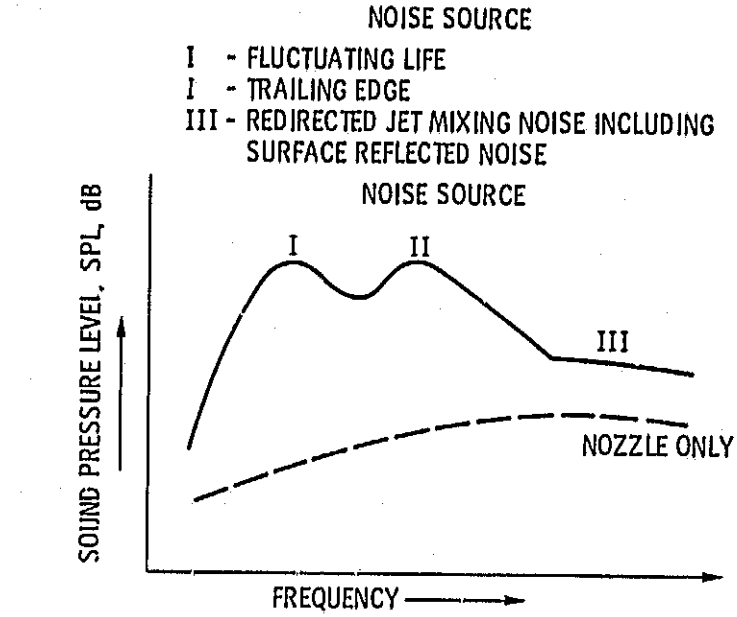

Figure 5. - Noise sources associated with OTW configurations.

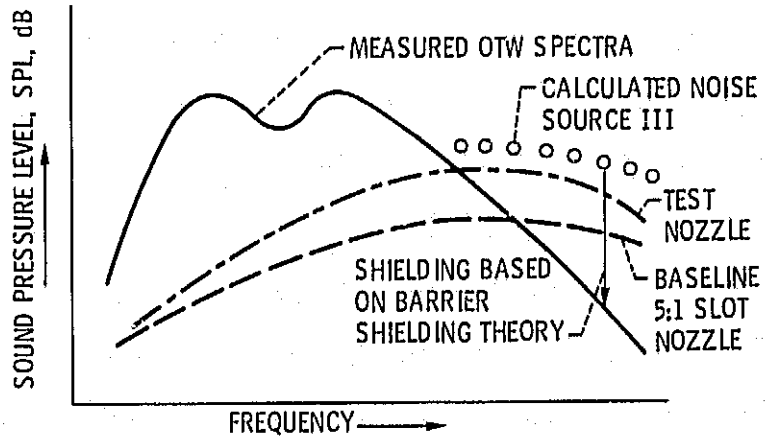

Figure 6. - Typical reconstituted noise source III using barrier shielding theory.

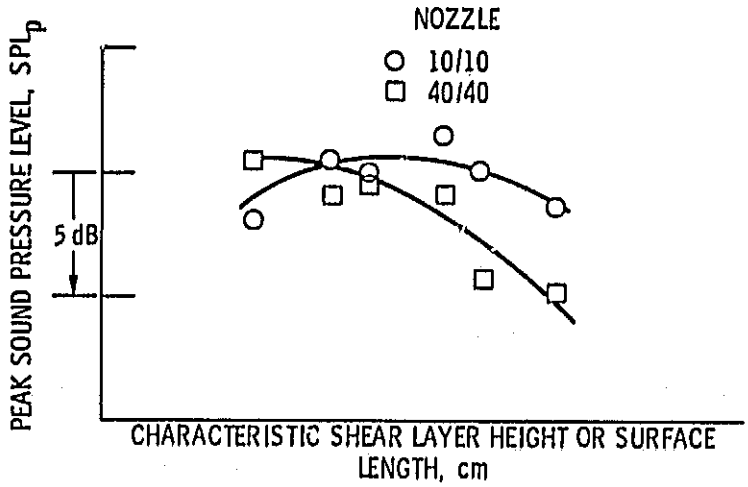

Figure 7. - Representative data trends of the peak SPL values for jet-surface interaction noise sources I and II; 20^0 flap angle; M_j, 0.83.

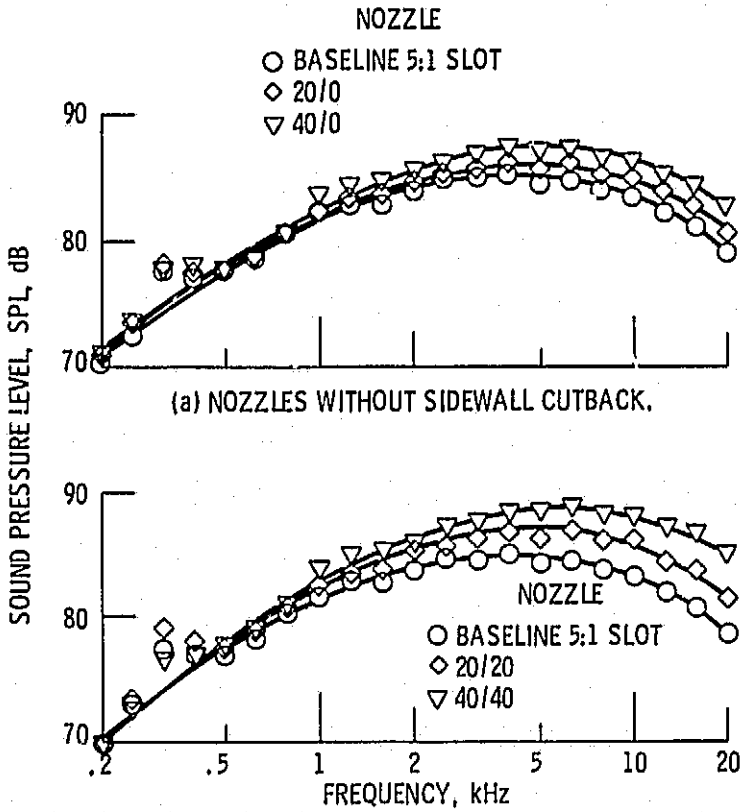

(b) NOZZLES WITH SIDEWALL CUTBACK.

Figure 8. - Representative spectra for nozzle only operation; M_j, 0.803.

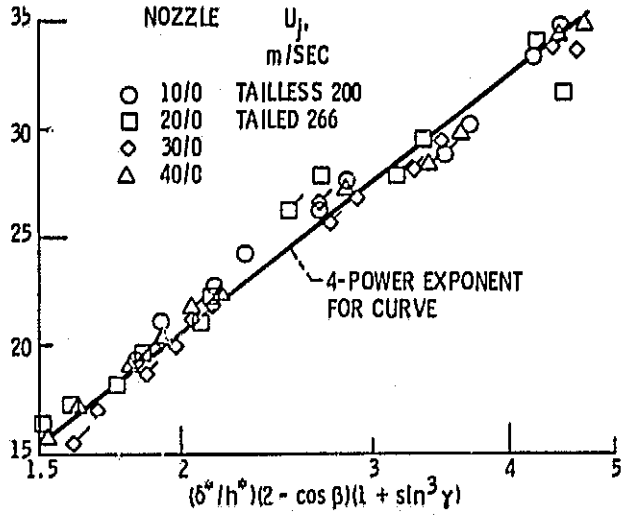

(a) NOZZLES WITHOUT SIDEWALL CUTBACK; 20° FLAP ANGLE.

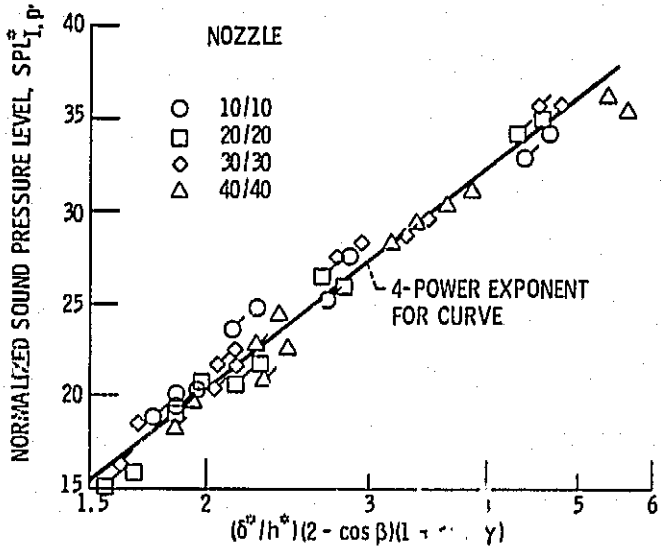

(b) NOZZLES WITH SIDEWALL CUTBACK; 20° FLAP ANGLE.

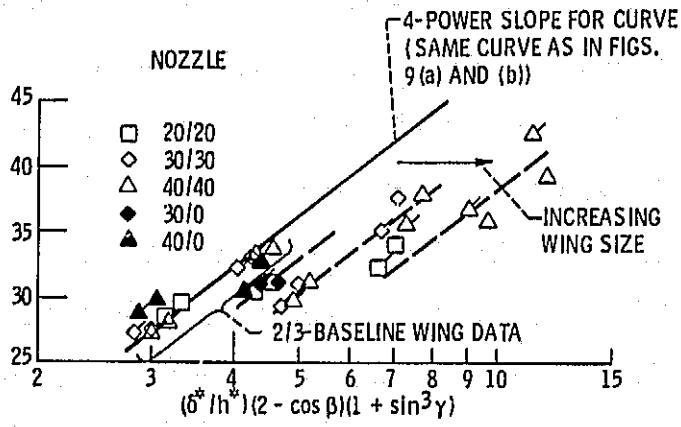

(c) NOZZLES WITH AND WITHOUT SIDEWALL CUTBACK; 60° FLAP ANGLE.

Figure 9. - Peak SPL correlation for noise source I.

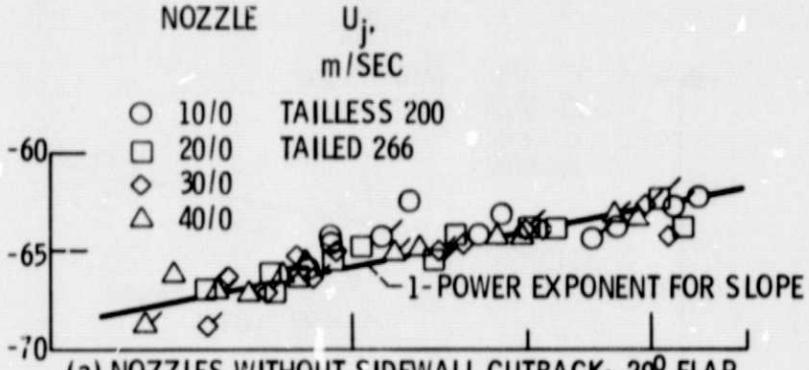

(a) NOZZLES WITHOUT SIDEWALL CUTBACK; 20° FLAP ANGLE.

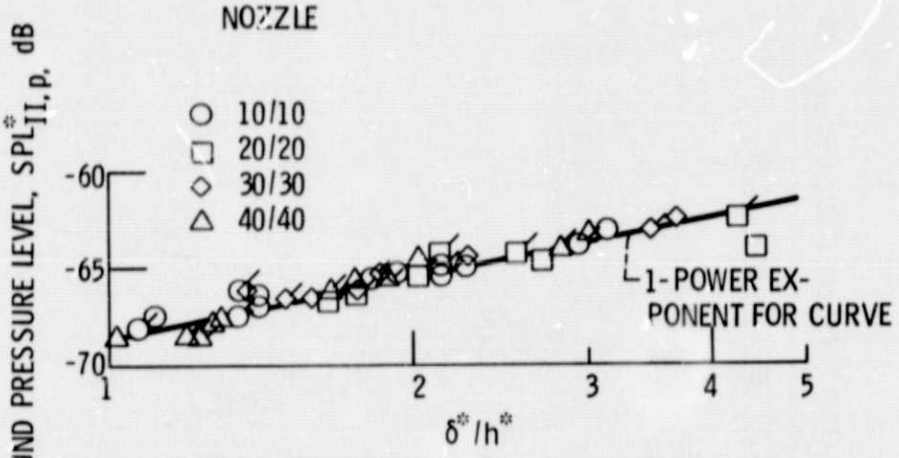

(b) NOZZLES WITH SIDEWALL CUTBACK; 20° FLAP ANGLE.

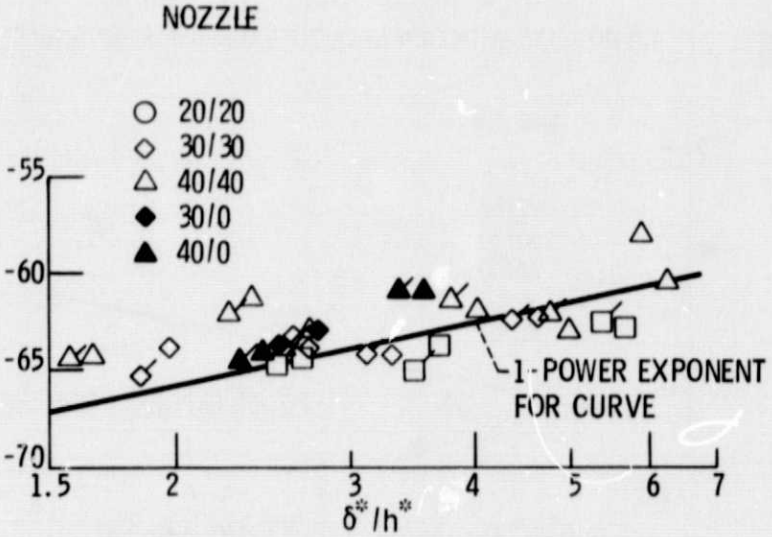

(c) NOZZLES WITH AND WITHOUT SIDEWALL CUTBACK; 60° FLAP ANGLE.

Figure 10. - Peak SPL correlation for noise source II.

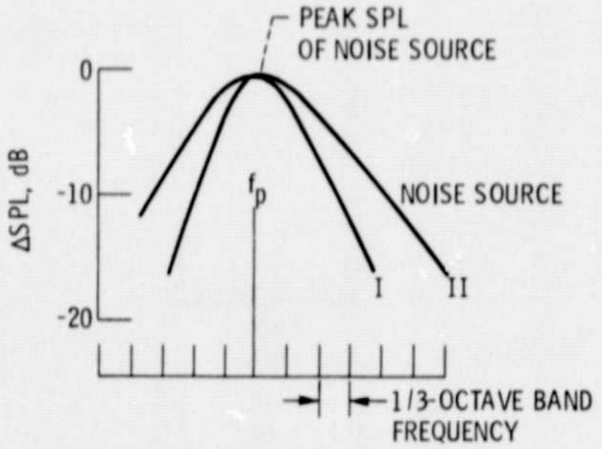

Figure 12. - Generalized noise source I and II spectra.

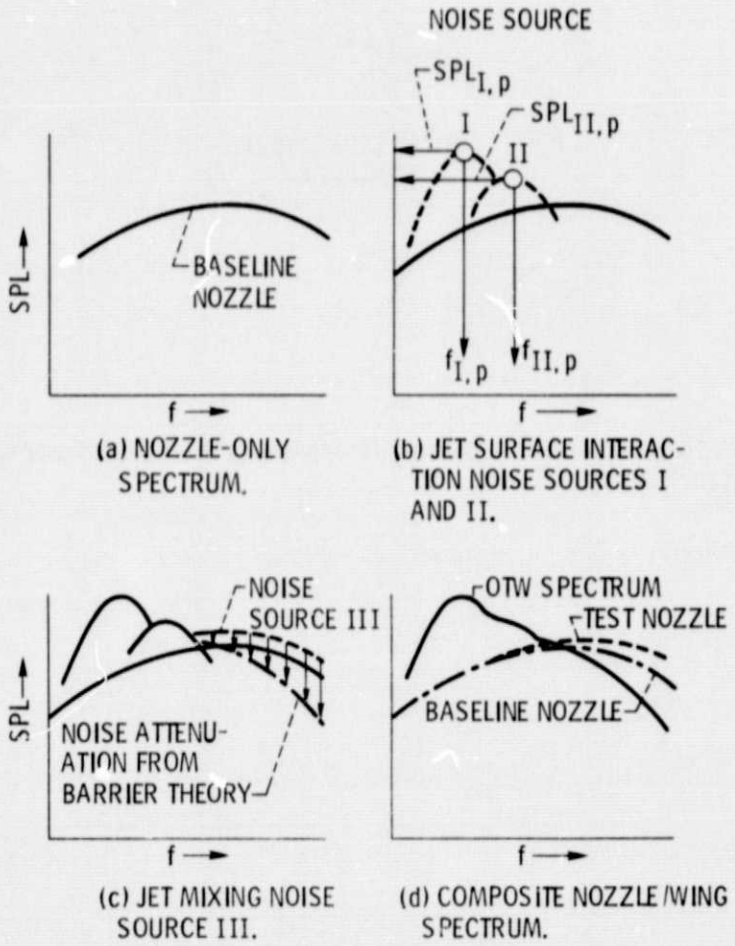

Figure 13. - Steps in development of OTW spectrum by method of superposition.

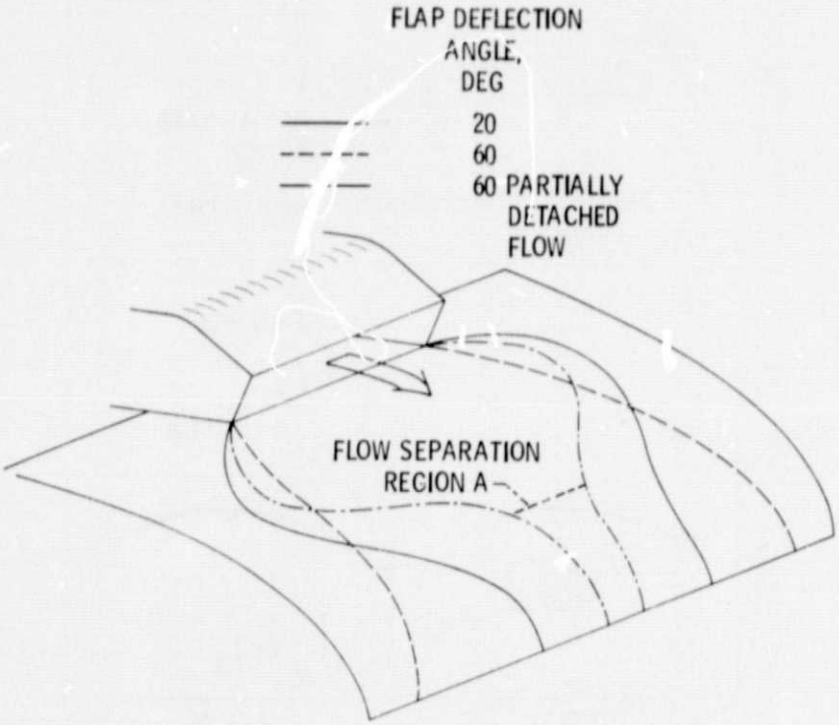

Figure 14. - Schematic sketch of representative jet flow patterns over wing/flap surface; M_j, 0.8.